

Estimating Risk and Uncertainty in Deep Reinforcement Learning

William R. Clements¹ Benoît-Marie Robaglia¹ Bastien Van Delft¹

Reda Babi Slaoui^{1,2} Sébastien Toth¹

¹Indust.ai, Paris, France

²Ecole des Ponts Paristech, Champs-sur-Marne, France

Abstract

We propose a method for disentangling epistemic and aleatoric uncertainties in deep reinforcement learning. Aleatoric uncertainty, or risk, which arises from inherently stochastic environments or agents, must be accounted for in the design of risk-sensitive algorithms. Epistemic uncertainty, which stems from limited data, is important both for risk-sensitivity and for efficient exploration. Our method combines elements from distributional reinforcement learning and approximate Bayesian inference techniques with neural networks, allowing us to disentangle both types of uncertainty on the expected return of a policy. Specifically, the learned return distribution provides the aleatoric uncertainty, and the Bayesian posterior yields the epistemic uncertainty. Although our approach in principle requires a large number of samples from the Bayesian posterior to estimate the epistemic uncertainty, we show that two networks already yield a useful approximation. We perform experiments that illustrate our method and some applications.

Reinforcement learning algorithms are exposed to two types of uncertainty: *aleatoric* uncertainty and *epistemic* uncertainty [Knight, 2012]. Aleatoric uncertainty, or risk, is uncertainty that stems from inherent randomness of the environment, which may be characterized. Epistemic uncertainty is uncertainty stemming from imperfect knowledge of the environment, which may be decreased with more information.

Correspondence to: william.clements@indust.ai

Distinguishing between both types of uncertainty is important in reinforcement learning [Osband, 2016, Moerland et al., 2017, Nikolov et al., 2019]. With the epistemic uncertainty, exploring a new environment can be done more efficiently, since actions can be taken to identify and better explore poorly known states. However, aleatoric risk can be irrelevant or even damaging [Russo and Van Roy, 2014] for exploration. Conversely, when designing risk-aware policies, the aleatoric risk can be more informative than the epistemic uncertainty, since a description of the environmental uncertainty can allow planning for all possible outcomes. Conflating both types of uncertainty can lead to inadequate exploration or risk-awareness [Osband, 2016].

We propose a method for disentangling aleatoric risk and epistemic uncertainty on the expected return of a policy, which is applicable to both stochastic and deterministic environments. Our method builds on the distributional reinforcement learning framework, which aims to learn the entire return distribution instead of only its expected value [Bellemare et al., 2017], and current methods for approximate Bayesian deep learning. Our main contributions are 1) a theoretical framework within which epistemic and aleatoric uncertainties can be separately estimated within distributional reinforcement learning, 2) a method for cheaply estimating both types of uncertainty using two networks, and 3) a demonstration that these uncertainties can successfully be used in complex reinforcement learning tasks

This paper is structured as follows. In sections 1 and 2, we discuss prior work on measuring uncertainties in reinforcement learning. Section 3 presents our framework for estimating both types of uncertainty on the expected return. Section 4 then experimentally illustrates our method for estimating these uncertainties and some of its applications.

1 RELATED WORK

Estimating both types of uncertainty is important for both model based and model free reinforcement learning. In model based reinforcement learning, uncertainties affect the predictions of a learned dynamics model of the environment. Uncertainty estimates can be used in planning, either for better exploration [Schmidhuber, 1991, Sun et al., 2011] or to avoid risky or unknown sections of the environment [Garcia and Fernández, 2015]. Model based algorithms that explicitly account for both aleatoric and epistemic uncertainties have recently been developed [Depeweg et al., 2018] and achieve state of the art results on some benchmarks [Chua et al., 2018, Henaff et al., 2019].

One approach that combines model free and model based techniques consists of using the uncertainties derived from a learned dynamics model to inform the policy of a model-free agent. The epistemic uncertainty associated with the learned model can for example be used as an intrinsic motivation bonus [Stadie et al., 2015, Pathak et al., 2017, Burda et al., 2019]. However, uncertainties on the transition model do not typically convey information about the uncertainty of the expected return of a policy, which is a quantity of fundamental interest in reinforcement learning.

A more direct approach for uncertainty estimation in model free reinforcement learning involves estimating the uncertainty of the expected return of a policy. This is the approach that we concern ourselves with. The epistemic uncertainty on the expected return has been shown to be useful for exploration [Osband et al., 2016, Azizzadenesheli et al., 2018, Touati et al., 2019]. On the other hand, the aleatoric uncertainty of the expected return is useful for designing risk-averse policies [Howard and Matheson, 1972, Tamar et al., 2016, Dabney et al., 2018a]. Distributional reinforcement learning algorithms have been developed that aim to learn the entire distribution of the returns, corresponding to the aleatoric uncertainty [Morimura et al., 2010, Bellemare et al., 2017]. However, these lines of work typically study either aleatoric uncertainty or epistemic uncertainty. [Tang and Agrawal, 2018, Moerland et al., 2017] do consider both types of uncertainty, but their methods yield only an aggregate uncertainty measure. [Nikolov et al., 2019] separately estimate both types of uncertainty to drive an exploration method based on information-directed sampling [Russo and Van Roy, 2014]. However,

in the absence of a single method for estimating both types of uncertainty they separately use bootstrapped DQN [Osband et al., 2016] to estimate epistemic uncertainty and distributional DQN [Bellemare et al., 2017] for the aleatoric uncertainty. Our work aims to provide a single framework for simultaneously estimating both uncertainties for the return distribution.

Outside of reinforcement learning, both types of uncertainties have for example been considered in computer vision [Kendall and Gal, 2017]. Closest to our method is the work of [Tagasovska and Lopez-Paz, 2019], where aleatoric uncertainty is measured using quantile estimates and epistemic uncertainty is measured with “orthonormal certificates” using a single network with multiple outputs. However, these two uncertainty estimates come from two different frameworks and are not necessarily commensurate, which limits their usefulness for measuring the uncertainty of the expected return in reinforcement learning.

2 BACKGROUND

We consider a discounted Markov Decision Process (MDP) defined by (χ, A, R, P, γ) , in which χ and A represent the state and action spaces, R is the distribution of rewards associated with performing actions given the states, P is the probability of transitioning between states given the actions, and γ is the discount factor.

Distributional reinforcement learning aims to learn the distribution of rewards $Z^\pi(s, a)$ associated with taking action a in state s and then following a policy π . This reward distribution can be learned using dynamic programming with the Bellman operator \mathcal{T} [Bellemare et al., 2017],

$$\mathcal{T}Z^\pi(s, a) \stackrel{D}{=} R(s, a) + \gamma Z^\pi(s', a') \quad (1)$$

where $\stackrel{D}{=}$ denotes that both distributions have equal probability laws, s' is distributed according to $P(\cdot|s, a)$, and a' is chosen according to π . A Bellman optimality operator \mathcal{T}' for the return distribution can also be defined as

$$\begin{aligned} \mathcal{T}'Z(s, a) &\stackrel{D}{=} R(s, a) + \gamma Z(s', a'), \\ \text{where } a' &\sim \text{argmax}_{a'} \mathbb{E}[Z(s', a')] \end{aligned} \quad (2)$$

where s' is distributed according to $P(\cdot|s, a)$. The Bellman optimality operator can be used to learn an optimal policy over an MDP, which then consists of always picking the action with the highest expected return.

Distributional reinforcement learning has several advantages compared to algorithms such as DQN [Mnih et al., 2015] that aim to learn only the expectation value of the returns. By learning the return distribution, distributional reinforcement learning can be used to account for risk [Dabney et al., 2018a]. Moreover, learning the return distribution instead of only its expectation value has been shown to lead on its own to improved performance on reinforcement learning benchmarks [Bellemare et al., 2017, Dabney et al., 2018b], and can lead to greater robustness to hyperparameter choices [Barth-Maron et al., 2018].

2.1 QUANTILE DISTRIBUTIONAL REINFORCEMENT LEARNING

Distributional reinforcement learning algorithms parameterize the return distribution in different ways. Whereas [Bellemare et al., 2017] use a categorical parameterization using a fixed number of atoms, which requires knowing the support of the return distribution in advance. [Dabney et al., 2018b] propose using a quantile parameterization using a fixed number of quantiles.

In this framework, a probability distribution $Z(s, a)$ is parameterized by N quantiles, and for each quantile $\tau_i = i/(N+1)$ for $i \in [1, N]$ of $Z(s, a)$ we aim to learn the corresponding quantile value $q_i(s, a)$. We denote as $\mathbf{q} = (q_1, \dots, q_N)$ the vector of these quantile estimates. Learning the quantile values proceeds by minimizing the quantile regression loss [Koenker and Hallock, 2001],

$$\mathcal{L}_q(\mathbf{q}) = \mathbb{E}_{z \sim Z(s, a)} \sum_{i=1}^N \rho_{\tau_i}(z - q_i(s, a)) \quad (3)$$

$$\text{where } \rho_{\tau_i}(u) = u \times (\tau_i - \mathbb{1}_{u < 0})$$

This loss can be minimized stochastically for each new value z sampled from $Z(s, a)$.

For temporal difference learning, $Z(s, a)$ is replaced with the Bellman target $R(s, a) + \gamma Z(s', a')$ as per equation 1 for the evaluation setting, or equation 2 for the control setting. The loss is thus

$$\mathcal{L}_{TD}(\mathbf{q}) = \mathbb{E}_{R(s, a)} \left[\frac{1}{N} \sum_{i=1}^N \sum_{j=1}^N \rho_{\tau_i}(\delta_{i,j}) \right] \quad (4)$$

$$\text{where } \left\{ \begin{array}{l} \rho_{\tau_i}(\delta_{i,j}) = \delta_{i,j} \times (\tau_i - \mathbb{1}_{\delta_{i,j} < 0}) \\ \delta_{i,j} = R(s, a) + \gamma q_j(s', a') - q_i(s, a) \end{array} \right.$$

In [Dabney et al., 2018b], the quantile regression DQN (QR-DQN) algorithm uses either the strict

quantile loss of equation 4 or a modified quantile Huber loss that is smooth at 0; we focus on the strict quantile loss since the quantile Huber loss produces biased quantile estimates.

3 ESTIMATING BOTH UNCERTAINTIES

Here, we show how both types of uncertainty on the expected return can be disentangled within distributional RL. We focus on the quantile formulation since such a parameterization does not assume a specific support for the returns and has empirically been shown to outperform the categorical parameterization of [Bellemare et al., 2017] on Atari benchmarks.

3.1 EPISTEMIC UNCERTAINTY ON QUANTILES

Bayesian inference provides a principled approach for quantifying epistemic uncertainties. We thus start by framing learning the quantiles of the return distribution as a Bayesian inference problem.

We consider state s , action a taken in state s , policy π , and data D consisting of K samples (z_1, \dots, z_K) from $Z^\pi(s, a)$. To learn the value of a given quantile τ of $Z^\pi(s, a)$, we consider the use of a neural network with parameters θ , which returns a value $y(\theta, s, a)$. We interpret possible values of θ as different hypotheses about the function relating the state-action pair to the value of quantile τ of $Z^\pi(s, a)$ [MacKay, 2003]. A Bayesian approach requires defining a prior on parameters θ ; we consider a normal prior θ centered around 0. Following [Yu and Moyeed, 2001], we also define a likelihood based on how well the output of the network matches the data using an asymmetric Laplace distribution,

$$P(D|\theta) = \prod_{j=1}^K f_\tau(z_j - y(\theta, s, a)) \quad (5)$$

$$\text{where } f_\tau(u) = \frac{\tau(1-\tau)}{\sigma_D} \exp\left(-\frac{\rho_\tau(u)}{\sigma_D}\right)$$

where σ_D is a characteristic length scale and ρ_τ is the same as in equation 3. With some assumptions, it can be shown that this choice of likelihood is consistent even when the actual distribution of the data is different from that assumed by this choice of likelihood [Sriram et al., 2013].

To estimate the entire return distribution instead of a single quantile, we extend this formalism to a network with N outputs $y_i(\theta, s, a)$, where each output

i is trained to learn the value of quantile τ_i . We thus define the likelihood

$$P(D|\boldsymbol{\theta}) = \prod_{j=1}^K \prod_{i=1}^N f_{\tau_i}(z_j - y_i(\boldsymbol{\theta}, s, a)) \quad (6)$$

Since each output of the network corresponds to an estimate of each quantile of the return distribution, we expect to have $y_i(\boldsymbol{\theta}, s, a) \geq y_j(\boldsymbol{\theta}, s, a)$ if $i \geq j$. Our choice of likelihood does indeed attribute higher likelihood to ordered quantiles than it does to disordered quantiles.

We now connect this inference problem to the neural network training loss described in the previous section. Minimizing the loss in equation 3 is equivalent to maximizing the likelihood in equation 6. Furthermore, with a normal prior on $\boldsymbol{\theta}$ with mean 0 and standard deviation σ_p , finding maximum a posteriori (MAP) parameters for the neural network is equivalent to minimizing the regularized quantile loss

$$\mathcal{L}_{reg}(\boldsymbol{\theta}) = \mathcal{L}_q(\mathbf{y}(\boldsymbol{\theta}, s, a)) + \sigma^2 \|\boldsymbol{\theta}\|^2 \quad (7)$$

where $\mathbf{y} = (y_1, \dots, y_N)$ and $\sigma = \frac{\sigma_D}{2\sigma_p}$.

3.2 UNCERTAINTY ESTIMATES

Framing learning the quantiles of the return distribution as a Bayesian inference problem gives us the tools for separately estimating both aleatoric and epistemic uncertainties.

3.2.1 Epistemic uncertainty

We start by considering the epistemic uncertainty on the estimation of a single quantile i . Having framed learning the value of this quantile as a Bayesian inference problem, we can now use any one of several methods for estimating epistemic uncertainties in neural networks. For instance, variance inference methods such as Bayes by Backprop [Blundell et al., 2015] and dropout [Gal and Ghahramani, 2016] can be used to draw samples from an approximate posterior distribution $P(\boldsymbol{\theta}|D)$ over neural network weights $\boldsymbol{\theta}$. Alternatively, samples from an approximate posterior can also be drawn using randomized MAP sampling [Pearce et al., 2018]. The variance of the outputs of the network with weights repeatedly sampled with these methods, $\text{var}_{\boldsymbol{\theta} \sim P(\boldsymbol{\theta}|D)}(y_i(\boldsymbol{\theta}, s, a))$, provides an estimate of the epistemic uncertainty of quantile i .

Instead of having separate epistemic uncertainty measurements on each quantile, it can be useful in reinforcement learning to have a single measure of

the epistemic uncertainty on the return distribution. We propose to obtain such a measure by aggregating the epistemic uncertainties on all quantiles,

$$\sigma_{\text{epistemic}}^2 = \mathbb{E}_{i \sim \mathcal{U}\{1, N\}} [\text{var}_{\boldsymbol{\theta} \sim P(\boldsymbol{\theta}|D)}(y_i(\boldsymbol{\theta}, s, a))] \quad (8)$$

where $\mathcal{U}\{1, N\}$ is the uniform distribution over integers from 1 to N . Note that since we measure the variance over $P(\boldsymbol{\theta}|D)$ separately for each quantile, potential correlations introduced between quantiles due to the presence of shared parameters $\boldsymbol{\theta}$ do not affect $\sigma_{\text{epistemic}}$. However, these correlations will have an impact when we consider using a small number of samples to estimate $\text{var}_{\boldsymbol{\theta} \sim P(\boldsymbol{\theta}|D)}(y_i(\boldsymbol{\theta}, s, a))$ and will be discussed later.

3.2.2 Aleatoric uncertainty

We define the aleatoric uncertainty as the variance of the expected value of the quantiles according to the posterior distribution over $\boldsymbol{\theta}$,

$$\sigma_{\text{aleatoric}}^2 = \text{var}_{i \sim \mathcal{U}\{1, N\}} [\mathbb{E}_{\boldsymbol{\theta} \sim P(\boldsymbol{\theta}|D)} y_i(\boldsymbol{\theta}, s, a)] \quad (9)$$

When considering only point estimates for $\boldsymbol{\theta}$, we recover a natural definition of aleatoric uncertainty as the variance of the quantiles.

3.2.3 Decomposition of Uncertainties

We require that the total uncertainty on the return distribution can be decomposed as the sum of these two uncertainties. We consider the total variance of the return distribution $\text{var}_{\boldsymbol{\theta} \sim P(\boldsymbol{\theta}|D), i \sim \mathcal{U}\{1, N\}}(y_i(\boldsymbol{\theta}, s, a))$, which for notational simplicity we write $\text{var}_{\boldsymbol{\theta}, i}(y_i(\boldsymbol{\theta}, s, a))$. We show in the appendix that the total variance can indeed be decomposed as follows,

$$\text{var}_{\boldsymbol{\theta}, i}(y_i(\boldsymbol{\theta}, s, a)) = \sigma_{\text{epistemic}}^2 + \sigma_{\text{aleatoric}}^2 \quad (10)$$

We also consider two limit cases as sanity checks. First, in the absence of data, there is nothing to distinguish between different quantiles and thus $\text{var}_{\boldsymbol{\theta}, i}(y_i(\boldsymbol{\theta}, s, a)) = \sigma_{\text{epistemic}}^2$. All the uncertainty is epistemic. In the limit of infinite data, the variance over $\boldsymbol{\theta}$ is zero and $\text{var}_{\boldsymbol{\theta}, i}(y_i(\boldsymbol{\theta}, s, a)) = \sigma_{\text{aleatoric}}^2$.

3.3 APPROXIMATE UNCERTAINTIES USING TWO NETWORKS

Estimating the variance and expectation over $\boldsymbol{\theta}$ in the previous expressions for both uncertainties requires in principle a large number of samples of $\boldsymbol{\theta}$, which is impractical. Instead, we propose the following approximations of $\sigma_{\text{epistemic}}^2$ and $\sigma_{\text{aleatoric}}^2$ using

only two samples $\boldsymbol{\theta}_A$ and $\boldsymbol{\theta}_B$ from the posterior distribution over $\boldsymbol{\theta}$,

$$\begin{aligned}\tilde{\sigma}_{\text{epistemic}}^2 &= \frac{1}{2} \mathbb{E}_{i \sim \mathcal{U}\{1, N\}} [(y_i(\boldsymbol{\theta}_A, s, a) - y_i(\boldsymbol{\theta}_B, s, a))^2] \\ \tilde{\sigma}_{\text{aleatoric}}^2 &= \text{cov}_{i \sim \mathcal{U}\{1, N\}} (y_i(\boldsymbol{\theta}_A, s, a), y_i(\boldsymbol{\theta}_B, s, a))\end{aligned}\quad (11)$$

In the appendix, we show that $\tilde{\sigma}_{\text{epistemic}}$ and $\tilde{\sigma}_{\text{aleatoric}}$ are unbiased estimators of $\sigma_{\text{epistemic}}$ and $\sigma_{\text{aleatoric}}$. Moreover, assuming that the network outputs are uncorrelated, we also show that the variance of these estimators converges towards 0 as the number of quantiles increases, and provide experimental evidence that a few tens of quantiles is sufficient to achieve relatively low variance.

Our result on the variance of these estimators does rely on the assumption that the network outputs are uncorrelated. Indeed, correlations between outputs could cause for example a network to overestimate *all* the quantiles. If both networks A and B produce overestimations, then $\tilde{\sigma}_{\text{epistemic}}$ would probably underestimate $\sigma_{\text{epistemic}}$. However, in the limit of infinite width Bayesian neural networks are uncorrelated for normal priors and separable likelihoods [Neal, 1995]. Moreover, in the appendix we show on a toy problem that for a large enough width, a network with several outputs does yield roughly the same range of predictions as an equivalent number of identical networks. These results suggest that, although imperfect, uncertainty estimates derived from two sufficiently large networks are still informative.

In figure 1, we provide an illustration of the uncertainties measured with $\tilde{\sigma}_{\text{epistemic}}$ and $\tilde{\sigma}_{\text{aleatoric}}$ on a toy dataset. We consider a deep neural network with parameters $\boldsymbol{\theta}$ that estimates 50 quantiles from the target distribution, and we draw two samples of $\boldsymbol{\theta}$ using approximate MAP sampling [Pearce et al., 2018]. As expected, $\tilde{\sigma}_{\text{epistemic}}$ is small close to the data but large far from the data, while $\tilde{\sigma}_{\text{aleatoric}}$ correctly captures the noise in the data.

3.4 DISTRIBUTIONAL Q-LEARNING WITH UNCERTAINTY ESTIMATES

Until now, we have been mainly concerned with learning the return distribution given an ensemble of samples of this distribution. Here, we discuss how our uncertainty estimate can be adapted to temporal difference learning of the return distribution. First, we replace the empirical return distribution with the Bellman target $\{\mathcal{T}Z(s, a)\}_{(s, a)}$ defined in equation 1 for the estimation setting, and in equation 2 for the

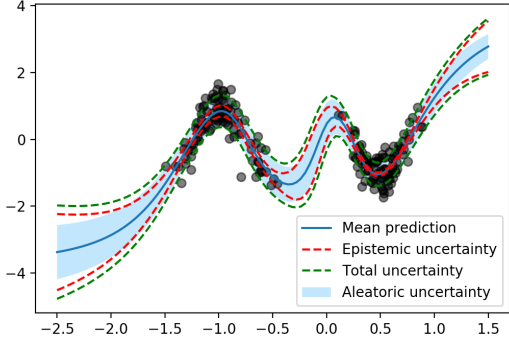


Figure 1: Illustration of uncertainty estimates provided by $\tilde{\sigma}_{\text{epistemic}}$ and $\tilde{\sigma}_{\text{aleatoric}}$ on a toy dataset (black dots). Intervals represent $\pm\sigma$ for all uncertainties, and the estimated total uncertainty $\tilde{\sigma}_{\text{total}}$ is defined as $\tilde{\sigma}_{\text{total}}^2 = \tilde{\sigma}_{\text{aleatoric}}^2 + \tilde{\sigma}_{\text{epistemic}}^2$.

control setting. By interpreting each quantile value of the target distribution as a sample drawn from the target distribution, we can now write the likelihood associated with the quantile estimates,

$$P(D|\boldsymbol{\theta}) \propto \exp(-\mathcal{L}_{TD}(\boldsymbol{\theta})) \quad (12)$$

where D now refers to the targets and \mathcal{L}_{TD} is the TD loss defined in equation 4. Since we are now working with networks sampled with different values of $\boldsymbol{\theta}$, a natural question is which quantile value(s) to use for the Bellman targets. We find that taking the mean over the samples of $\boldsymbol{\theta}$ of the quantile values works well in practice.

4 EXPERIMENTS

We first compare our epistemic uncertainty estimate to alternative epistemic uncertainty metrics for neural networks using a stochastic contextual bandit problem. We then illustrate applications of our uncertainty estimates for different algorithms in two reinforcement learning environments: Cartpole and the Atari suite.

Unless otherwise indicated, in the following uncertainties are estimated with $\tilde{\sigma}_{\text{epistemic}}$ and $\tilde{\sigma}_{\text{aleatoric}}$ using samples from the posterior distribution over $\boldsymbol{\theta}$ drawn using the approximate MAP sampling procedure of [Pearce et al., 2018]. Code to reproduce these experiments is available at <https://github.com/IndustAI/risk-and-uncertainty>.

4.1 A CONTEXTUAL BANDIT PROBLEM

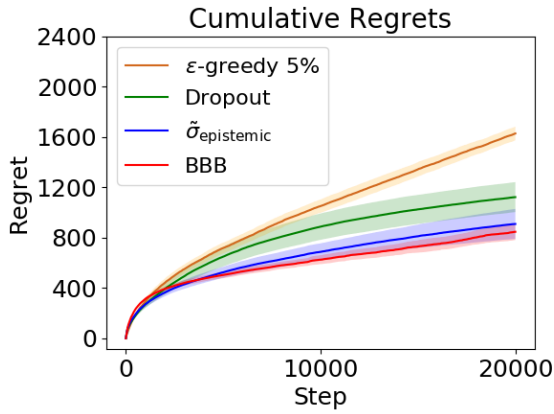


Figure 2: Regret accumulated by different agents on a contextual bandit problem: an ϵ -greedy agent (yellow), and three agents that select actions with Thompson sampling and different epistemic uncertainty metrics. Green: Dropout [Gal and Ghahramani, 2016]. Blue: Our method with $\tilde{\sigma}_{\text{epistemic}}$. Red: Bayes by Backprop [Blundell et al., 2015]. Shaded areas correspond to the 95% confidence interval of the mean.

Directly comparing different neural network epistemic uncertainty estimates derived from different theoretical frameworks is difficult, because they usually rely on different approximations or assumptions. We thus propose an indirect comparison between epistemic uncertainties measured with $\tilde{\sigma}_{\text{epistemic}}$ and other established epistemic uncertainty measures on a contextual stochastic bandit problem. We use a variation of the problem presented in [Guez, 2015, Blundell et al., 2015], in which at each step an agent is shown a mushroom, characterized by a set of features, and must decide to eat it or not. The agent is penalized for eating a toxic mushroom and rewarded for eating an edible mushroom, and must learn to distinguish good from bad mushrooms from their features.

Figure 2 shows the cumulative regret achieved by several agents on this task. One agent uses $\tilde{\sigma}_{\text{epistemic}}$ and samples from the approximate posterior over θ using randomized MAP sampling [Pearce et al., 2018]. One agent uses Bayes-by-Backprop [Blundell et al., 2015], while another agent uses variational dropout [Gal and Ghahramani, 2016]. These three agents select actions with Thompson sampling (see ap-

pendix for details). One baseline agent simply uses a fixed ϵ -greedy policy. We see that the agent that uses $\tilde{\sigma}_{\text{epistemic}}$ is competitive with the other agents that use other established neural networks epistemic uncertainty metrics, which indicates that $\tilde{\sigma}_{\text{epistemic}}$ does provide meaningful uncertainty estimates.

4.2 APPLICATIONS IN REINFORCEMENT LEARNING

We now study applications of our uncertainty quantification method in reinforcement learning.

4.2.1 Improved Exploration

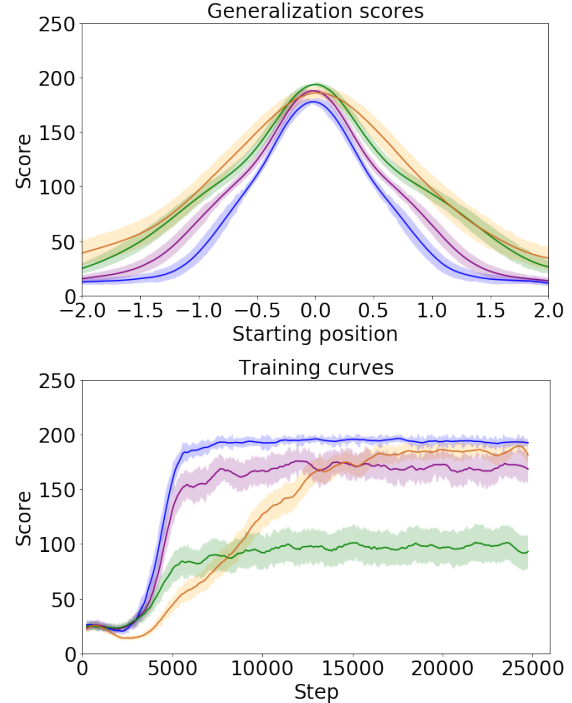


Figure 3: Experimental results for generalization in Cartpole, for an agent that uses $\tilde{\sigma}_{\text{epistemic}}$ with Thompson sampling and several ϵ -greedy agents. Top: score achieved as a function of starting position over greedy rollouts. Bottom: training curves. Shaded areas correspond to 95% confidence intervals around the mean. Our agent is the only one that both generalizes well and converges to near-perfect scores during training.

As a first application, we show that our epistemic uncertainty estimate allows distributional reinforcement learning agents to efficiently explore

their environment, leading to improved generalization. We use the OpenAI Gym domain Cartpole [Brockman et al., 2016], in which the agent must keep a pole upright as long as possible on a cart that the agent can either move left or right. The episode terminates either after 200 time steps, if the cart leaves the track, or if the pole exceeds a certain angle. We measure generalization ability by training agents on the standard Cartpole domain in which the cart is initialized at the center of the track, and test them on modified domains in which the cart is initialized at different locations along the track.

Figure 3 compares the performance of the agent that chooses actions with Thompson sampling via $\tilde{\sigma}_{\text{epistemic}}$ to different ϵ -greedy agents. For all ϵ -greedy agents, ϵ is annealed during training over the first 5000 training steps; however the final value reached differs between agents. Our agent is the only one that both generalizes well and converges to near-perfect scores during training. We notice that training is slower than for greedy agents, which combined with the higher generalization scores is consistent with our agent spending more time exploring its environment. We note that this link between enhanced exploration and generalization has been observed before for example in [Witty et al., 2018].

4.2.2 Information Directed Sampling

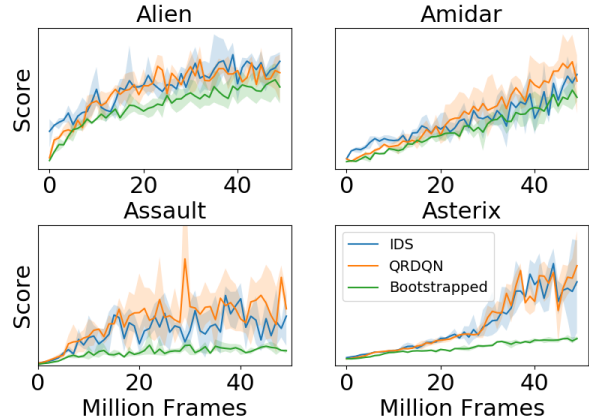


Figure 4: Evaluation results during training of different agents on four Atari games. Blue: agent using Information-Directed Sampling (IDS) with $\tilde{\sigma}_{\text{epistemic}}$ and $\tilde{\sigma}_{\text{aleatoric}}$. Orange: QR-DQN. Green: Bootstrapped DQN. Agents are evaluated every 1M training frames for 500k steps as in [Mnih et al., 2015]. Shaded areas represent min and max scores over 3 seeds.

Here, we demonstrate that our method for sepa-

rating both uncertainties can be used in a high-dimensional domain to drive information-directed sampling (IDS). In this scheme, proposed by [Nikolov et al., 2019] and shown to achieve good results on Atari games from the Arcade Learning Suite [Bellemare et al., 2013], the agent takes actions based on the ratio between the regret associated with the action and the information to be gained. Calculating this ratio requires estimates of both types of uncertainty (see appendix for details).

Whereas [Nikolov et al., 2019] estimate both types of uncertainty using Bootstrapped DQN [Osband et al., 2016] on the one hand and distributional reinforcement learning with a categorical parameterization on the other, we propose to use instead a quantile parameterization and our uncertainty estimates $\tilde{\sigma}_{\text{epistemic}}$ and $\tilde{\sigma}_{\text{aleatoric}}$. As a proof of principle experiment, we train an agent that uses these uncertainties to drive information-directed sampling on 4 Atari games. We also train two baseline agents: a QR-DQN agent as in [Dabney et al., 2018b], and a bootstrapped DQN agent as in [Osband et al., 2016]. Due to computational limitations, we restrict our training procedure to 50 million training frames instead of the usual 200 million.

Experimental results are shown in figure 4. We see that the agent that uses $\tilde{\sigma}_{\text{epistemic}}$ and $\tilde{\sigma}_{\text{aleatoric}}$ outperforms bootstrapped DQN and is competitive with QR-DQN. These results demonstrate that our uncertainty estimates can successfully be used for information-directed sampling on complex domains. However, interestingly we do not observe an advantage of our implementation of IDS over QR-DQN, which warrants an explanation. First, this result is consistent with the results from [Nikolov et al., 2019], whose implementation of IDS outperforms QR-DQN in only 30 out of 55 games, and indicates that QR-DQN is a very strong baseline. Moreover, as the QR-DQN implementation of [Dabney et al., 2018b] uses a 1% epsilon-greedy policy for most of training, we can expect only marginal gains from improved exploration on games where QR-DQN already performs well.

4.2.3 Tracking epistemic uncertainties

Lastly, we show that our uncertainty metrics can be used to identify novel situations encountered by the agent. For this experiment, we train an agent with the QR-DQN algorithm as in [Dabney et al., 2018b] with an ϵ -greedy policy on Breakout, using a modified architecture that allows us to measure $\tilde{\sigma}_{\text{epistemic}}$

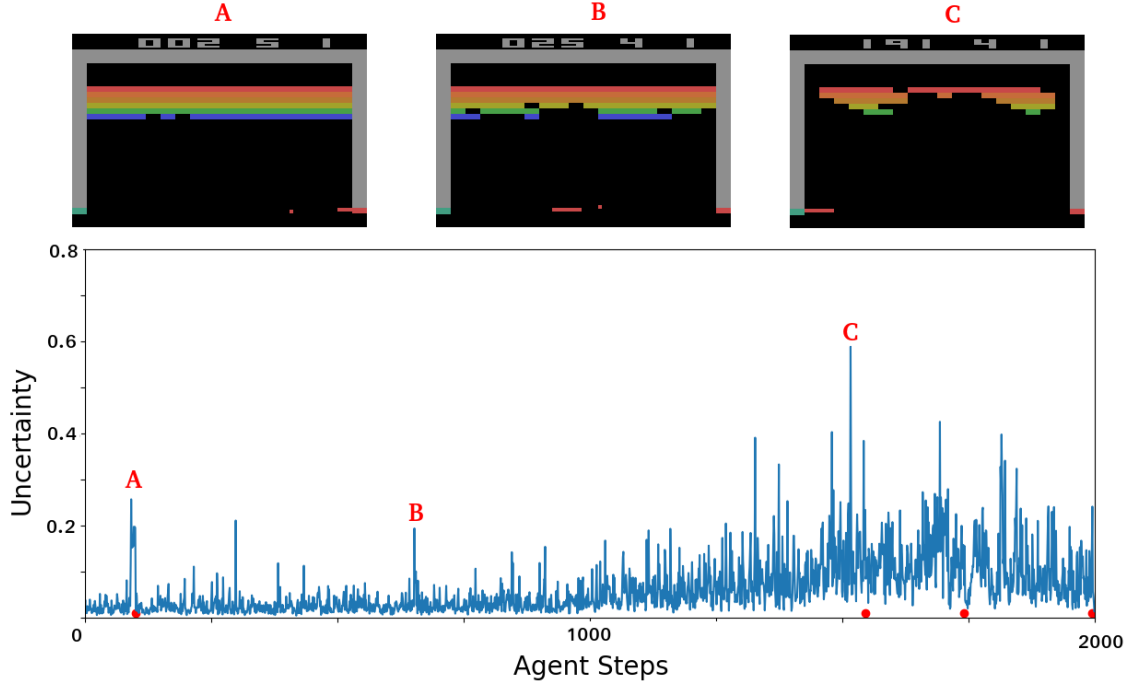


Figure 5: Epistemic uncertainty on a distributional agent’s actions over the course of an episode of Breakout. Loss of life is indicated as a red dot along the x-axis. Salient game frames can be identified from increases in uncertainty. A) The agent’s ϵ -greedy policy causes it to reach states it cannot recover from and lose a life. This does not happen often for a trained agent, hence the agent’s surprise. B) The agent almost misses the ball. C) Due to faulty rendering in Breakout, here the ball is hidden behind the top-right bricks, hence the very high uncertainty for this state.

and $\tilde{\sigma}_{\text{aleatoric}}$. We then monitor the agent’s epistemic uncertainty over a test episode in which it follows a 5% ϵ -greedy policy, which forces it to sometimes make mistakes.

The trained agent’s epistemic uncertainty over the course of an episode is shown in figure 5. The uncertainty behaves in the way we would expect it to; in addition to the specific spikes in uncertainty pointed out in the figure that we can easily interpret, we also observe that the agent’s uncertainty generally increases during an episode. This is because the agent encounters a wider variety of possible states at the end of an episode than at its start. Monitoring an agent’s uncertainty in this way in complex domains would be valuable for real-life reinforcement learning agents, for example to detect and prevent potential accidents.

5 CONCLUSION

Estimating both aleatoric and epistemic uncertainty is important for developing agents that can both explore efficiently and account for risk in their actions.

We propose a scheme whereby both types of uncertainty on the expected return of a policy can be estimated in deep reinforcement learning. Our approach combines distributional reinforcement learning and approximate Bayesian inference methods for neural networks. We also show that estimators for these uncertainties can be obtained using only two networks. Our experimental results in the Cartpole and Atari domains illustrate applications of our method.

References

- [Azizzadenesheli et al., 2018] Azizzadenesheli, K., Brunskill, E., and Anandkumar, A. (2018). Efficient exploration through Bayesian deep Q-networks. *Information Theory and Applications Workshop*.
- [Bache and Lichman, 2013] Bache, K. and Lichman, M. (2013). UCI machine learning repository.
- [Barth-Maron et al., 2018] Barth-Maron, G., Hoffman, M. W., Budden, D., Dabney, W., Horgan, D., Muldal, A., Heess, N., and Lillicrap, T.

(2018). Distributed distributional deterministic policy gradients. In *International Conference on Learning Representations*.

[Bellemare et al., 2017] Bellemare, M. G., Dabney, W., and Munos, R. (2017). A distributional perspective on reinforcement learning. In *International Conference on Machine Learning*.

[Bellemare et al., 2013] Bellemare, M. G., Naddaf, Y., Veness, J., and Bowling, M. (2013). The arcade learning environment: an evaluation platform for general agents. *Journal of Artificial Intelligence Research*, 47:253–279.

[Blundell et al., 2015] Blundell, C., Cornebise, J., Kavukcuoglu, K., and Wierstra, D. (2015). Weight uncertainty in neural networks. In *International Conference on Machine Learning*, pages 1613–1622. JMLR. org.

[Brockman et al., 2016] Brockman, G., Cheung, V., Pettersson, L., Schneider, J., Schulman, J., Tang, J., and Zaremba, W. (2016). Openai gym. *arXiv preprint arXiv:1606.01540*.

[Burda et al., 2019] Burda, Y., Edwards, H., Storkey, A., and Klimov, O. (2019). Exploration by random network distillation. *International Conference on Learning Representations*.

[Chua et al., 2018] Chua, K., Calandra, R., McAlister, R., and Levine, S. (2018). Deep reinforcement learning in a handful of trials using probabilistic dynamics models. In *Neural Information Processing Systems*, pages 4754–4765.

[Dabney et al., 2018a] Dabney, W., Ostrovski, G., Silver, D., and Munos, R. (2018a). Implicit quantile networks for distributional reinforcement learning. *International Conference on Machine Learning*.

[Dabney et al., 2018b] Dabney, W., Rowland, M., Bellemare, M. G., and Munos, R. (2018b). Distributional reinforcement learning with quantile regression. In *AAAI Conference on Artificial Intelligence*.

[Depeweg et al., 2018] Depeweg, S., Hernandez-Lobato, J.-M., Doshi-Velez, F., and Udluft, S. (2018). Decomposition of uncertainty in bayesian deep learning for efficient and risk-sensitive learning. In *International Conference on Machine Learning*, pages 1192–1201.

[Gal and Ghahramani, 2016] Gal, Y. and Ghahramani, Z. (2016). Dropout as a Bayesian approximation: representing model uncertainty in deep learning. In *International Conference on Machine Learning*, pages 1050–1059.

[Garcia and Fernández, 2015] Garcia, J. and Fernández, F. (2015). A comprehensive survey on safe reinforcement learning. *Journal of Machine Learning Research*, 16(1):1437–1480.

[Guez, 2015] Guez, A. (2015). *Sample-based search methods for Bayes-adaptive planning*. PhD thesis, UCL (University College London).

[Hafner et al., 2018] Hafner, D., Tran, D., Irpan, A., Lillicrap, T., and Davidson, J. (2018). Reliable uncertainty estimates in deep neural networks using noise contrastive priors. *arXiv preprint arXiv:1807.09289*.

[Henaff et al., 2019] Henaff, M., Canziani, A., and LeCun, Y. (2019). Model-predictive policy learning with uncertainty regularization for driving in dense traffic. *International Conference on Learning Representations*.

[Howard and Matheson, 1972] Howard, R. A. and Matheson, J. E. (1972). Risk-sensitive markov decision processes. *Management science*, 18(7):356–369.

[Kendall and Gal, 2017] Kendall, A. and Gal, Y. (2017). What uncertainties do we need in Bayesian deep learning for computer vision? In *Neural Information Processing systems*, pages 5574–5584.

[Knight, 2012] Knight, F. H. (2012). *Risk, uncertainty and profit*. Courier Corporation.

[Koenker and Hallock, 2001] Koenker, R. and Hallock, K. F. (2001). Quantile regression. *Journal of economic perspectives*, 15(4):143–156.

[MacKay, 2003] MacKay, D. J. (2003). *Information theory, inference and learning algorithms*. Cambridge university press.

[Mnih et al., 2015] Mnih, V., Kavukcuoglu, K., Silver, D., Rusu, A. A., Veness, J., Bellemare, M. G., Graves, A., Riedmiller, M., Fidjeland, A. K., Ostrovski, G., et al. (2015). Human-level control through deep reinforcement learning. *Nature*, 518(7540):529.

[Moerland et al., 2017] Moerland, T. M., Broekens, J., and Jonker, C. M. (2017). Efficient exploration

with double uncertain value networks. In *Neural Information Processing Systems*.

[Morimura et al., 2010] Morimura, T., Sugiyama, M., Kashima, H., Hachiya, H., and Tanaka, T. (2010). Parametric return density estimation for reinforcement learning. In *Uncertainty in Artificial Intelligence*, pages 368–375. AUAI Press.

[Neal, 1995] Neal, R. M. (1995). *Bayesian learning for neural networks*, volume 118.

[Nikolov et al., 2019] Nikolov, N., Kirschner, J., Berkenkamp, F., and Krause, A. (2019). Information-directed exploration for deep reinforcement learning. *International Conference on Learning Representations*.

[Osband, 2016] Osband, I. (2016). Risk versus uncertainty in deep learning: Bayes, bootstrap and the dangers of dropout. In *NIPS 2016 Workshop on Bayesian Deep Learning*.

[Osband et al., 2016] Osband, I., Blundell, C., Pritzel, A., and Van Roy, B. (2016). Deep exploration via bootstrapped DQN. In *Neural Information Processing Systems*, pages 4026–4034.

[Pathak et al., 2017] Pathak, D., Agrawal, P., Efros, A. A., and Darrell, T. (2017). Curiosity-driven exploration by self-supervised prediction. In *International Conference on Machine Learning*.

[Pearce et al., 2018] Pearce, T., Zaki, M., Brintrup, A., Anastassacos, N., and Neely, A. (2018). Uncertainty in neural networks: Bayesian ensembling. *arXiv preprint arXiv:1810.05546*.

[Russo and Van Roy, 2014] Russo, D. and Van Roy, B. (2014). Learning to optimize via information-directed sampling. In *Neural Information Processing Systems*, pages 1583–1591.

[Schmidhuber, 1991] Schmidhuber, J. (1991). A possibility for implementing curiosity and boredom in model-building neural controllers. In *International conference on simulation of adaptive behavior: From animals to animats*, pages 222–227.

[Sriram et al., 2013] Sriram, K., Ramamoorthi, R., Ghosh, P., et al. (2013). Posterior consistency of Bayesian quantile regression based on the misspecified asymmetric Laplace density. *Bayesian Analysis*, 8(2):479–504.

[Stadie et al., 2015] Stadie, B. C., Levine, S., and Abbeel, P. (2015). Incentivizing exploration in reinforcement learning with deep predictive models. *NeurIPS 2015 Workshop on Deep Reinforcement Learning*.

[Sun et al., 2011] Sun, Y., Gomez, F., and Schmidhuber, J. (2011). Planning to be surprised: Optimal bayesian exploration in dynamic environments. In *International Conference on Artificial General Intelligence*, pages 41–51. Springer.

[Tagasovska and Lopez-Paz, 2019] Tagasovska, N. and Lopez-Paz, D. (2019). Single-model uncertainties for deep learning. In *Neural Information Processing Systems*, pages 6414–6425.

[Tamar et al., 2016] Tamar, A., Di Castro, D., and Mannor, S. (2016). Learning the variance of the reward-to-go. *The Journal of Machine Learning Research*, 17(1):361–396.

[Tang and Agrawal, 2018] Tang, Y. and Agrawal, S. (2018). Exploration by distributional reinforcement learning. *International Joint Conference on Artificial Intelligence*.

[Touati et al., 2019] Touati, A., Satija, H., Romoff, J., Pineau, J., and Vincent, P. (2019). Randomized value functions via multiplicative normalizing flows. *Uncertainty in Artificial Intelligence*.

[Witty et al., 2018] Witty, S., Ki Lee, J., Tosch, E., Atrey, A., Littman, M., and Jensen, D. (2018). Measuring and characterizing generalization in deep reinforcement learning. *arXiv preprint arXiv:1812.02868*.

[Yu and Moyeed, 2001] Yu, K. and Moyeed, R. A. (2001). Bayesian quantile regression. *Statistics & Probability Letters*, 54(4):437–447.

A Proofs

In the following, for notational simplicity we will omit the dependence of $y_i(\boldsymbol{\theta}, s, a)$ on s and a . Moreover, subscripts used in variances/expectation values should be interpreted as the variance/expectation value taken over the distribution of the variables in the subscript, so that for example $\mathbb{E}_{\boldsymbol{\theta}} = \mathbb{E}_{\boldsymbol{\theta} \sim P(\boldsymbol{\theta}|D)}$ and $\mathbb{E}_i = \mathbb{E}_{i \sim \mathcal{U}\{1, N\}}$. We will also assume that the following integrals over $P(\boldsymbol{\theta}|D)$ are well defined, which, considering in particular the Gaussian prior over the weights, is a reasonable assumption.

A.1 Sum of uncertainties

Here, we show that $\text{var}_{\boldsymbol{\theta},i}(y_i(\boldsymbol{\theta}, s, a)) = \sigma_{\text{epistemic}}^2 + \sigma_{\text{aleatoric}}^2$.

$$\begin{aligned} \text{var}_{\boldsymbol{\theta},i}(y_i(\boldsymbol{\theta})) &= \int_{\boldsymbol{\theta}} \frac{1}{N} \sum_{j=1}^N (y_j(\boldsymbol{\theta}) - \mathbb{E}_{\boldsymbol{\theta},i}[y_i(\boldsymbol{\theta})])^2 P(\boldsymbol{\theta}|D) d\boldsymbol{\theta} \\ &= \int_{\boldsymbol{\theta}} \frac{1}{N} \sum_{j=1}^N (y_j(\boldsymbol{\theta}) - \mathbb{E}_{\boldsymbol{\theta}}[y_j(\boldsymbol{\theta})] + \mathbb{E}_{\boldsymbol{\theta}}[y_j(\boldsymbol{\theta})] - \mathbb{E}_{\boldsymbol{\theta},i}[y_i(\boldsymbol{\theta})])^2 P(\boldsymbol{\theta}|D) d\boldsymbol{\theta} \\ &= \int_{\boldsymbol{\theta}} \frac{1}{N} \sum_{j=1}^N \left((y_j(\boldsymbol{\theta}) - \mathbb{E}_{\boldsymbol{\theta}}[y_j(\boldsymbol{\theta})])^2 \right. \\ &\quad \left. + (\mathbb{E}_{\boldsymbol{\theta}}[y_j(\boldsymbol{\theta})] - \mathbb{E}_{\boldsymbol{\theta},i}[y_i(\boldsymbol{\theta})])^2 \right. \\ &\quad \left. + 2(\mathbb{E}_{\boldsymbol{\theta}}[y_j(\boldsymbol{\theta})] - \mathbb{E}_{\boldsymbol{\theta},i}[y_i(\boldsymbol{\theta})])(y_j(\boldsymbol{\theta}) - \mathbb{E}_{\boldsymbol{\theta}}[y_j(\boldsymbol{\theta})]) \right) P(\boldsymbol{\theta}|D) d\boldsymbol{\theta} \end{aligned}$$

The integral over $\boldsymbol{\theta}$ of the last line is 0, which leaves us with

$$\begin{aligned} \text{var}_{\boldsymbol{\theta},i}(y_i(\boldsymbol{\theta})) &= \int_{\boldsymbol{\theta}} \frac{1}{N} \sum_{j=1}^N (y_j(\boldsymbol{\theta}) - \mathbb{E}_{\boldsymbol{\theta}}[y_j(\boldsymbol{\theta})])^2 P(\boldsymbol{\theta}|D) d\boldsymbol{\theta} + \int_{\boldsymbol{\theta}} \frac{1}{N} \sum_{j=1}^N (\mathbb{E}_{\boldsymbol{\theta}}[y_j(\boldsymbol{\theta})] - \mathbb{E}_{\boldsymbol{\theta},i}[y_i(\boldsymbol{\theta})])^2 P(\boldsymbol{\theta}|D) d\boldsymbol{\theta} \\ &= \frac{1}{N} \sum_{j=1}^N \int_{\boldsymbol{\theta}} (y_j(\boldsymbol{\theta}) - \mathbb{E}_{\boldsymbol{\theta}}[y_j(\boldsymbol{\theta})])^2 P(\boldsymbol{\theta}|D) d\boldsymbol{\theta} + \frac{1}{N} \sum_{j=1}^N (\mathbb{E}_{\boldsymbol{\theta}}[y_j(\boldsymbol{\theta})] - \mathbb{E}_{\boldsymbol{\theta},i}[y_i(\boldsymbol{\theta})])^2 \\ &= \mathbb{E}_i(\text{var}_{\boldsymbol{\theta}}(y_i(\boldsymbol{\theta}))) + \text{var}_i(\mathbb{E}_{\boldsymbol{\theta}} y_i(\boldsymbol{\theta})) \\ &= \sigma_{\text{epistemic}}^2 + \sigma_{\text{aleatoric}}^2 \end{aligned}$$

A.2 Approximate uncertainties using two networks

A.2.1 Bias of the estimators

Here, we show that $\tilde{\sigma}_{\text{epistemic}}$ and $\tilde{\sigma}_{\text{aleatoric}}$ are unbiased estimators of $\sigma_{\text{epistemic}}$ and $\sigma_{\text{aleatoric}}$. In the following, $\mathbb{E}_{\boldsymbol{\theta}_A, \boldsymbol{\theta}_B}$ indicates the expectation value when $\boldsymbol{\theta}_A$ and $\boldsymbol{\theta}_B$ are drawn from the posterior distribution over $\boldsymbol{\theta}$. Moreover, in what follows it can easily be verified that expectations over $\boldsymbol{\theta}$ and over i are interchangeable due to the discrete nature of the expectation over i .

$$\begin{aligned} \mathbb{E}_{\boldsymbol{\theta}_A, \boldsymbol{\theta}_B}[\tilde{\sigma}_{\text{epistemic}}^2] &= \frac{1}{2} \mathbb{E}_{\boldsymbol{\theta}_A, \boldsymbol{\theta}_B} \mathbb{E}_i[(y_i(\boldsymbol{\theta}_A) - y_i(\boldsymbol{\theta}_B))^2] \\ &= \frac{1}{2} \mathbb{E}_{\boldsymbol{\theta}_A, \boldsymbol{\theta}_B} \mathbb{E}_i[(y_i(\boldsymbol{\theta}_A) - \mathbb{E}_{\boldsymbol{\theta}}(y_i(\boldsymbol{\theta})) + \mathbb{E}_{\boldsymbol{\theta}}(y_i(\boldsymbol{\theta})) - y_i(\boldsymbol{\theta}_B))^2] \\ &= \frac{1}{2} \mathbb{E}_{\boldsymbol{\theta}_A, \boldsymbol{\theta}_B} [\mathbb{E}_i[(y_i(\boldsymbol{\theta}_A) - \mathbb{E}_{\boldsymbol{\theta}}(y_i(\boldsymbol{\theta})))^2] + \mathbb{E}_i[(\mathbb{E}_{\boldsymbol{\theta}}(y_i(\boldsymbol{\theta})) - y_i(\boldsymbol{\theta}_B))^2]] \\ &\quad + 2 \mathbb{E}_i[((\mathbb{E}_{\boldsymbol{\theta}}(y_i(\boldsymbol{\theta}))) - y_i(\boldsymbol{\theta}_B))(y_i(\boldsymbol{\theta}_A) - \mathbb{E}_{\boldsymbol{\theta}}(y_i(\boldsymbol{\theta})))]] \end{aligned}$$

The average over either $\boldsymbol{\theta}_A$ or $\boldsymbol{\theta}_B$ of the last line is zero, which, after noticing that $\boldsymbol{\theta}_A$ and $\boldsymbol{\theta}_B$ are now separable such that we can use the equality $\mathbb{E}_{\boldsymbol{\theta}_A}[y_i(\boldsymbol{\theta}_A)] = \mathbb{E}_{\boldsymbol{\theta}_B}[y_i(\boldsymbol{\theta}_B)] = \mathbb{E}_{\boldsymbol{\theta}}[y_i(\boldsymbol{\theta})]$, leaves us with

$$\begin{aligned}\mathbb{E}_{\boldsymbol{\theta}_A, \boldsymbol{\theta}_B}[\tilde{\sigma}_{\text{epistemic}}^2] &= \frac{1}{2} (\mathbb{E}_{\boldsymbol{\theta}} [\mathbb{E}_i(y_i(\boldsymbol{\theta}) - \mathbb{E}_{\boldsymbol{\theta}}(y_i(\boldsymbol{\theta})))^2 + \mathbb{E}_i(\mathbb{E}_{\boldsymbol{\theta}}(y_i(\boldsymbol{\theta})) - y_i(\boldsymbol{\theta}))^2]) \\ &= \mathbb{E}_{\boldsymbol{\theta}} [\mathbb{E}_i(y_i(\boldsymbol{\theta}) - \mathbb{E}_{\boldsymbol{\theta}}(y_i(\boldsymbol{\theta})))^2] \\ &= \mathbb{E}_i [\mathbb{E}_{\boldsymbol{\theta}}(y_i(\boldsymbol{\theta}) - \mathbb{E}_{\boldsymbol{\theta}}(y_i(\boldsymbol{\theta})))^2] \\ &= \mathbb{E}_i [\text{var}_{\boldsymbol{\theta}}(y_i(\boldsymbol{\theta}))] \\ &= \sigma_{\text{epistemic}}^2\end{aligned}$$

so $\tilde{\sigma}_{\text{epistemic}}$ is indeed an unbiased estimator of $\sigma_{\text{epistemic}}$.

Similarly, for $\tilde{\sigma}_{\text{aleatoric}}$, and introducing $\epsilon_i(\boldsymbol{\theta}_A) = y_i(\boldsymbol{\theta}_A) - \mathbb{E}_{\boldsymbol{\theta}}(y_i(\boldsymbol{\theta}))$ and $\epsilon_i(\boldsymbol{\theta}_B) = y_i(\boldsymbol{\theta}_B) - \mathbb{E}_{\boldsymbol{\theta}}(y_i(\boldsymbol{\theta}))$,

$$\begin{aligned}\mathbb{E}_{\boldsymbol{\theta}_A, \boldsymbol{\theta}_B}[\tilde{\sigma}_{\text{aleatoric}}^2] &= \mathbb{E}_{\boldsymbol{\theta}_A, \boldsymbol{\theta}_B} \text{cov}_i(y_i(\boldsymbol{\theta}_A), y_i(\boldsymbol{\theta}_B)) \\ &= \mathbb{E}_{\boldsymbol{\theta}_A, \boldsymbol{\theta}_B} \text{cov}_i(\epsilon_i(\boldsymbol{\theta}_A) + \mathbb{E}_{\boldsymbol{\theta}}(y_i(\boldsymbol{\theta})), \epsilon_i(\boldsymbol{\theta}_B) + \mathbb{E}_{\boldsymbol{\theta}}(y_i(\boldsymbol{\theta}))) \\ &= \mathbb{E}_{\boldsymbol{\theta}_A, \boldsymbol{\theta}_B} [\text{cov}_i(\mathbb{E}_{\boldsymbol{\theta}}(y_i(\boldsymbol{\theta})), \mathbb{E}_{\boldsymbol{\theta}}(y_i(\boldsymbol{\theta}))) + \text{cov}_i(\epsilon_i(\boldsymbol{\theta}_A), \mathbb{E}_{\boldsymbol{\theta}}(y_i(\boldsymbol{\theta}))) \\ &\quad + \text{cov}_i(\mathbb{E}_{\boldsymbol{\theta}}(y_i(\boldsymbol{\theta})), \epsilon_i(\boldsymbol{\theta}_B)) + \text{cov}_i(\epsilon_i(\boldsymbol{\theta}_A), \epsilon_i(\boldsymbol{\theta}_B))]\end{aligned}$$

Looking at these terms individually, we have

$$\begin{aligned}\mathbb{E}_{\boldsymbol{\theta}_A, \boldsymbol{\theta}_B} [\text{cov}_i(\mathbb{E}_{\boldsymbol{\theta}}(y_i(\boldsymbol{\theta})), \mathbb{E}_{\boldsymbol{\theta}}(y_i(\boldsymbol{\theta})))] &= \text{var}_i(\mathbb{E}_{\boldsymbol{\theta}}(y_i(\boldsymbol{\theta}))) \\ &= \sigma_{\text{aleatoric}}^2\end{aligned}$$

$$\begin{aligned}\mathbb{E}_{\boldsymbol{\theta}_A, \boldsymbol{\theta}_B} [\text{cov}_i(\epsilon_i(\boldsymbol{\theta}_A), \mathbb{E}_{\boldsymbol{\theta}}(y_i(\boldsymbol{\theta})))] &= \mathbb{E}_{\boldsymbol{\theta}_A} [\text{cov}_i(\epsilon_i(\boldsymbol{\theta}_A), \mathbb{E}_{\boldsymbol{\theta}}(y_i(\boldsymbol{\theta})))] \\ &= \mathbb{E}_{\boldsymbol{\theta}_A} \left[\frac{1}{N} \sum_{j=1}^N (\epsilon_j(\boldsymbol{\theta}_A) - \mathbb{E}_i(\epsilon_i(\boldsymbol{\theta}_A))) (\mathbb{E}_{\boldsymbol{\theta}}(y_j(\boldsymbol{\theta})) - \mathbb{E}_i \mathbb{E}_{\boldsymbol{\theta}}(y_i(\boldsymbol{\theta}))) \right] \\ &= \frac{1}{N} \sum_{j=1}^N (\mathbb{E}_{\boldsymbol{\theta}}(y_j(\boldsymbol{\theta})) - \mathbb{E}_i \mathbb{E}_{\boldsymbol{\theta}}(y_i(\boldsymbol{\theta}))) (\mathbb{E}_{\boldsymbol{\theta}_A}(\epsilon_j(\boldsymbol{\theta}_A)) - \mathbb{E}_i(\mathbb{E}_{\boldsymbol{\theta}_A}(\epsilon_i(\boldsymbol{\theta}_A)))) \\ &= 0 \quad \text{since } \mathbb{E}_{\boldsymbol{\theta}_A}(\epsilon_i(\boldsymbol{\theta}_A)) = 0 \quad \text{for all } i\end{aligned}$$

$$\mathbb{E}_{\boldsymbol{\theta}_A, \boldsymbol{\theta}_B} [\text{cov}_i(\mathbb{E}_{\boldsymbol{\theta}}(y_i(\boldsymbol{\theta}))), \epsilon_i(\boldsymbol{\theta}_B)] = 0 \quad [\text{Same derivation as previous expression}]$$

$$\begin{aligned}\mathbb{E}_{\boldsymbol{\theta}_A, \boldsymbol{\theta}_B} [\text{cov}_i(\epsilon_i(\boldsymbol{\theta}_A), \epsilon_i(\boldsymbol{\theta}_B))] &= \mathbb{E}_{\boldsymbol{\theta}_A, \boldsymbol{\theta}_B} \left[\frac{1}{N} \sum_{j=1}^N (\epsilon_j(\boldsymbol{\theta}_A) - \mathbb{E}_i(\epsilon_i(\boldsymbol{\theta}_A))) (\epsilon_j(\boldsymbol{\theta}_B) - \mathbb{E}_i(\epsilon_i(\boldsymbol{\theta}_B))) \right] \\ &= \mathbb{E}_{\boldsymbol{\theta}_A} \left[\frac{1}{N} \sum_{j=1}^N (\epsilon_j(\boldsymbol{\theta}_A) - \mathbb{E}_i(\epsilon_i(\boldsymbol{\theta}_A))) (\mathbb{E}_{\boldsymbol{\theta}_B}(\epsilon_j(\boldsymbol{\theta}_B)) - \mathbb{E}_i(\mathbb{E}_{\boldsymbol{\theta}_B}(\epsilon_i(\boldsymbol{\theta}_B)))) \right] \\ &= 0\end{aligned}$$

As desired, we end up with

$$\mathbb{E}_{\boldsymbol{\theta}_A, \boldsymbol{\theta}_B}[\tilde{\sigma}_{\text{aleatoric}}^2] = \sigma_{\text{aleatoric}}^2$$

A.3 Variance of the estimators

Using the same notation as in the previous section, we can write

$$\begin{aligned}\text{var}_{\boldsymbol{\theta}_A, \boldsymbol{\theta}_B} [\tilde{\sigma}_{\text{epistemic}}^2] &= \frac{1}{4} \text{var}_{\boldsymbol{\theta}_A, \boldsymbol{\theta}_B} \mathbb{E}_i [(y_i(\boldsymbol{\theta}_A) - y_i(\boldsymbol{\theta}_B))^2] \\ &= \frac{1}{4} \text{var}_{\boldsymbol{\theta}_A, \boldsymbol{\theta}_B} \left[\frac{1}{N} \sum_{i=1}^N (y_i(\boldsymbol{\theta}_A) - y_i(\boldsymbol{\theta}_B))^2 \right] \\ &= \frac{1}{4N^2} \text{var}_{\boldsymbol{\theta}_A, \boldsymbol{\theta}_B} \left[\sum_{i=1}^N (y_i(\boldsymbol{\theta}_A) - y_i(\boldsymbol{\theta}_B))^2 \right]\end{aligned}$$

We now require our assumption that all outputs of the neural networks are decorrelated to write

$$\begin{aligned}\text{var}_{\boldsymbol{\theta}_A, \boldsymbol{\theta}_B} [\tilde{\sigma}_{\text{epistemic}}^2] &= \frac{1}{4N^2} \sum_{i=1}^N \text{var}_{\boldsymbol{\theta}_A, \boldsymbol{\theta}_B} [(y_i(\boldsymbol{\theta}_A) - y_i(\boldsymbol{\theta}_B))^2] \\ &= \frac{1}{4N^2} \sum_{i=1}^N \text{var}_{\boldsymbol{\theta}_A, \boldsymbol{\theta}_B} [y_i(\boldsymbol{\theta}_A)^2 + y_i(\boldsymbol{\theta}_B)^2 + 2y_i(\boldsymbol{\theta}_A)y_i(\boldsymbol{\theta}_B)] \\ &\leq \frac{3}{4N^2} \sum_{i=1}^N [\text{var}_{\boldsymbol{\theta}_A, \boldsymbol{\theta}_B} [y_i(\boldsymbol{\theta}_A)^2] + \text{var}_{\boldsymbol{\theta}_A, \boldsymbol{\theta}_B} [y_i(\boldsymbol{\theta}_B)^2] + 4\text{var}_{\boldsymbol{\theta}_A, \boldsymbol{\theta}_B} [y_i(\boldsymbol{\theta}_A)y_i(\boldsymbol{\theta}_B)]] \\ &\quad [\text{Where we used the Cauchy-Schwartz inequality}] \\ &\leq \frac{3}{4N^2} \sum_{i=1}^N [2\text{var}_{\boldsymbol{\theta}} [y_i(\boldsymbol{\theta})^2] + 8(\mathbb{E}_{\boldsymbol{\theta}} y_i(\boldsymbol{\theta}))^2 \text{var}_{\boldsymbol{\theta}} [y_i(\boldsymbol{\theta})] + 2(\text{var}_{\boldsymbol{\theta}} [y_i(\boldsymbol{\theta})])^2]\end{aligned}$$

We now further assume that $\mathbb{E}_{\boldsymbol{\theta}} [y_i(\boldsymbol{\theta})]$, $\text{var}_{\boldsymbol{\theta}} [y_i(\boldsymbol{\theta})]$, and $\text{var}_{\boldsymbol{\theta}} [y_i^2(\boldsymbol{\theta})]$ are bounded for all i and N . Then, there is a constant C such that, for all i and N ,

$$2\text{var}_{\boldsymbol{\theta}} [y_i(\boldsymbol{\theta})^2] + 8(\mathbb{E}_{\boldsymbol{\theta}} [y_i(\boldsymbol{\theta})])^2 \text{var}_{\boldsymbol{\theta}} [y_i(\boldsymbol{\theta})] + 2(\text{var}_{\boldsymbol{\theta}} [y_i(\boldsymbol{\theta})])^2 \leq C$$

We then obtain

$$\begin{aligned}\text{var}_{\boldsymbol{\theta}_A, \boldsymbol{\theta}_B} [\tilde{\sigma}_{\text{epistemic}}^2] &\leq \frac{3}{4N^2} \sum_{i=1}^N C \\ &\leq \frac{C}{4N}\end{aligned}$$

The variance of $\tilde{\sigma}_{\text{epistemic}}^2$ (and thus that of $\tilde{\sigma}_{\text{epistemic}}$) therefore decreases towards 0 as the number of quantiles increases.

As for the aleatoric uncertainty, a similar bound can be derived by rewriting $\text{var}_{\boldsymbol{\theta}_A, \boldsymbol{\theta}_B} [\tilde{\sigma}_{\text{aleatoric}}^2]$ as follows.

$$\begin{aligned}\text{var}_{\boldsymbol{\theta}_A, \boldsymbol{\theta}_B} [\tilde{\sigma}_{\text{aleatoric}}^2] &= \text{var}_{\boldsymbol{\theta}_A, \boldsymbol{\theta}_B} [\text{cov}_i (y_i(\boldsymbol{\theta}_A), y_i(\boldsymbol{\theta}_B))] \\ &= \text{var}_{\boldsymbol{\theta}_A, \boldsymbol{\theta}_B} \left[\frac{1}{N} \sum_{j=1}^N (y_j(\boldsymbol{\theta}_A) - \mathbb{E}_i y_i(\boldsymbol{\theta}_A))(y_j(\boldsymbol{\theta}_B) - \mathbb{E}_i y_i(\boldsymbol{\theta}_B)) \right] \\ &= \frac{1}{N^2} \text{var}_{\boldsymbol{\theta}_A, \boldsymbol{\theta}_B} \left[\sum_{j=1}^N (y_j(\boldsymbol{\theta}_A) - \mathbb{E}_i y_i(\boldsymbol{\theta}_A))(y_j(\boldsymbol{\theta}_B) - \mathbb{E}_i y_i(\boldsymbol{\theta}_B)) \right]\end{aligned}$$

In a manner similar as for the derivation of the variance of $\tilde{\sigma}_{\text{epistemic}}^2$, assuming that the network outputs are uncorrelated and that the first moments of $y_i(\boldsymbol{\theta})$ are bounded, we can also derive a bound for $\text{var}_{\boldsymbol{\theta}_A, \boldsymbol{\theta}_B} [\tilde{\sigma}_{\text{aleatoric}}^2]$ that converges to 0 with increasing N .

B Thompson sampling using our epistemic uncertainty metric

Here we provide our method for selecting an action with Thompson sampling using our epistemic uncertainty estimate $\tilde{\sigma}_{\text{epistemic}}^2$, which we use for both our bandit experiment and our experiment on Cartpole. Thompson sampling in these contexts should be used with the epistemic uncertainty and not the aleatoric uncertainty; our method allows us to separate both contributions. Since we do not have access to the exact shape of the epistemic posterior distribution for the expectation of the returns, we approximate it with a normal distribution.

Algorithm 1 Action selection with Thompson sampling and our epistemic uncertainty estimate

Input: A set of possible actions \mathcal{A} and a method for drawing samples from the posterior distribution of the neural network parameters θ .

for a in \mathcal{A} **do**

- Obtain two sets of quantile estimates $\mathbf{y}(\theta_A)$ and $\mathbf{y}(\theta_B)$
- Calculate uncertainty $\tilde{\sigma}_{\text{epistemic}}^2$
- Calculate mean of quantiles $\mu = \frac{1}{2} \mathbb{E}_i[y_i(\theta_A) + y_i(\theta_B)]$
- Draw a sample \hat{Q}_a from $\mathcal{N}(\mu, \tilde{\sigma}_{\text{epistemic}}^2)$

end for

Output: $\text{argmax}_a[\hat{Q}_a]$

C Correlations between the outputs of a Bayesian neural network

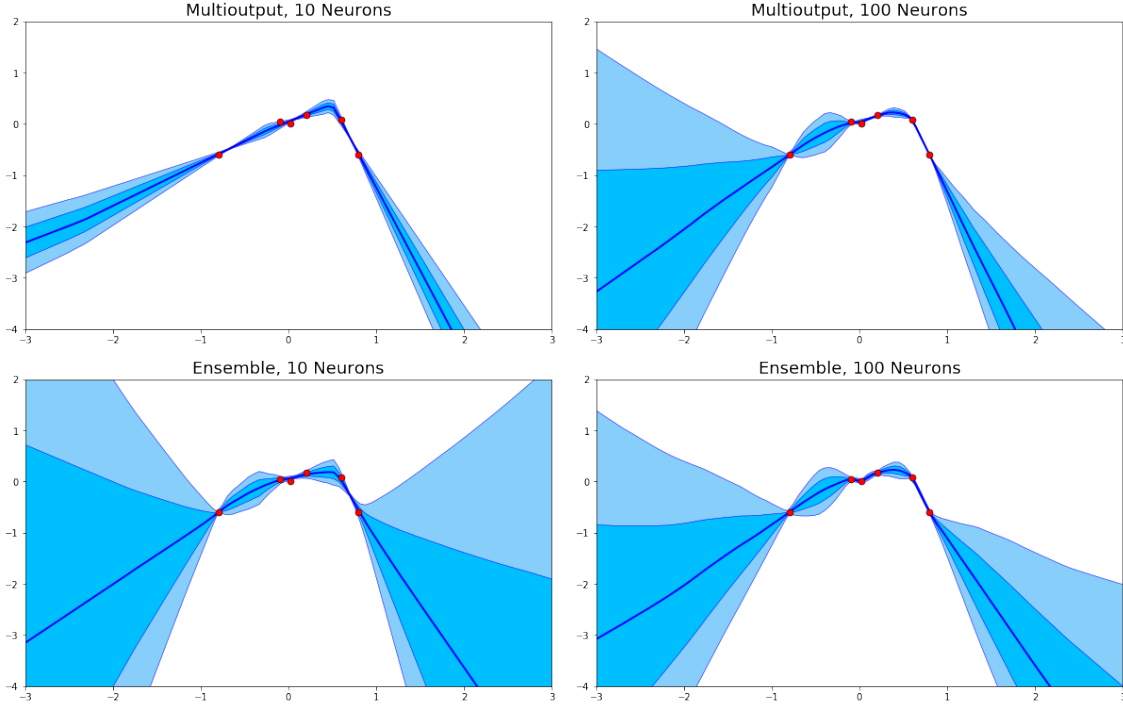


Figure 6: Comparison of epistemic uncertainties obtained with the approximate MAP sampling method of [Pearce et al., 2018]. Top: uncertainties obtained by a single neural network with twenty outputs. Bottom: uncertainties obtained by an ensemble of 20 networks. Left: 10 neurons per hidden layer. Right: 100 neurons per hidden layer. The two colors of shading represent one and two standard deviations from the mean.

In principle, in the limit of infinite width Bayesian neural networks are uncorrelated for normal priors and separable likelihoods [Neal, 1995]. Here, we experimentally explore in which cases this applies to finite width

neural networks and to approximate Bayesian techniques such as the randomized MAP sampling technique used in our work.

C.1 Uncertainties for different network widths

First, we compare the epistemic uncertainties produced by an ensemble of neural networks produced by the “anchoring” approximate MAP sampling technique of [Pearce et al., 2018] to that produced by a single neural network (also produced with approximate MAP sampling) with several outputs on a toy regression problem. Both the problem formulation and the code for this experiment draw from the work of [Pearce et al., 2018].

Representative samples from these experiments are shown in figure 6. For a small neural network with only 10 neurons per layer the different outputs of the multioutput neural network are indeed strongly correlated, which leads to poor uncertainty estimates (top left). The ensemble produces significantly better uncertainty estimates for the same network width (bottom left). However, as we increase the width of the neural network to 100 (top right) the uncertainty estimates of the network with multiple outputs improve and become close to those obtained by the larger ensemble of networks of the same width (bottom right).

C.2 Variance of $\tilde{\sigma}_{\text{epistemic}}^2$ and number of quantiles

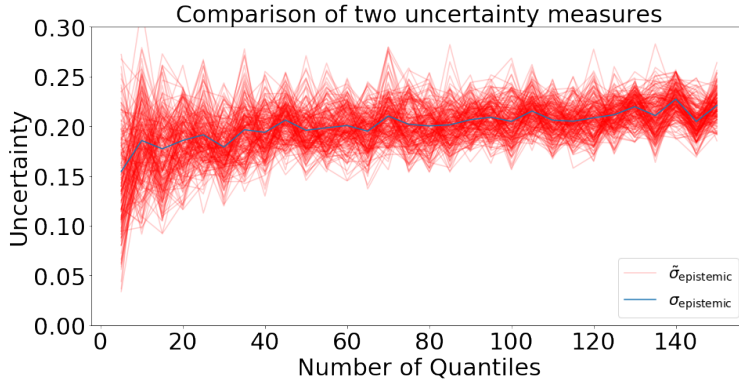


Figure 7: Comparison of $\tilde{\sigma}_{\text{epistemic}}^2$ to an estimate of $\sigma_{\text{epistemic}}^2$ estimated by an ensemble of twenty samples from an approximate posterior distribution over θ . Blue: estimate of $\sigma_{\text{epistemic}}^2$. Red: $\tilde{\sigma}_{\text{epistemic}}^2$, calculated for all pairs of θ in the ensemble.

We also empirically test the notion that $\tilde{\sigma}_{\text{epistemic}}^2$ provides a low variance estimate of $\sigma_{\text{epistemic}}^2$ with a reasonable number of quantiles. We obtain twenty samples of θ using the approximate MAP sampling technique of [Pearce et al., 2018], trained on a fixed set of samples from a standard normal distribution. We repeat this process for different numbers of quantiles. We then use this ensemble to measure epistemic uncertainty in two different ways. The first uncertainty measure is $\sigma_{\text{epistemic}}^2$, where the expectation over θ is estimated from our ensemble. The second uncertainty measure is $\tilde{\sigma}_{\text{epistemic}}^2$, which we calculate for all 190 pairs in this ensemble. Our results are shown in figure 7. We see that both uncertainty measures give the same result on average. $\tilde{\sigma}_{\text{epistemic}}^2$ has higher variance, but as the number of quantiles increases the variance decreases.

D Further information and results on the contextual bandit problem

Here, we provide more information and results on the contextual bandit experiment. Specific implementation details can be found in our code at <https://github.com/IndustAI/risk-and-uncertainty>.

D.1 Experiment setup

We use the UCI mushroom data set [Bache and Lichman, 2013], where each entry contains features about different mushrooms and whether they are edible or not. In a similar manner to [Blundell et al., 2015], we convert this dataset into a contextual bandit problem in which at each step an agent must choose between eating a given mushroom or not eating it. The agent receives stochastic rewards drawn from normal distributions with standard deviation 1, and means -3 and 1 for respectively eating a toxic mushroom and eating an edible mushroom. The agent receives a deterministic reward of 0 for not eating the mushroom.

Our agents all use neural networks to predict the reward or distribution of rewards corresponding to each action (eating or not eating), as a function of the mushroom’s features. Each neural network uses two hidden layers of 100 neurons each. Both the ϵ -greedy agent and the agent that uses Thompson sampling with $\tilde{\sigma}_{\text{epistemic}}$ are distributional with 50 quantiles to be learned, whereas the BBB and Dropout agents have a single regression target which is the mean squared error.

Each time an agent acts, its action as well as the corresponding reward is stored in memory. An important question is when and how often to update the parameters of the neural networks. Ideally, we would like to train the networks to convergence at every new observation. However, this is very impractical. After initial testing in which we compared the performance of neural networks updated with 100 batches of 32 samples from memory every ten steps and that of neural networks updated with a single batch at every step (where different learning rates for each approach were tried), we empirically found little difference between the two approaches and chose to update the network once at every step for our experiments.

In approximate Bayesian methods such as Bayes by Backprop, Dropout, and randomized MAP sampling it is important to remember that the weight of the likelihood with respect to the prior scales linearly with the amount of data. Correspondingly, for Bayes by Backprop and the randomized MAP sampling technique used to derive $\tilde{\sigma}_{\text{epistemic}}$, the weight of the prior is annealed linearly with the number of mushrooms in the replay buffer. Similarly, for dropout we tested several annealing schedules of the dropout parameter and kept the schedule that provided the best results.

The hyperparameters corresponding to learning rate, variance of the noise, and scale of the prior were separately optimized for each agent to achieve the lowest cumulative regret. Each experiment was repeated over at least 20 random seeds to obtain a reasonably small confidence interval of the mean.

D.2 Additional results

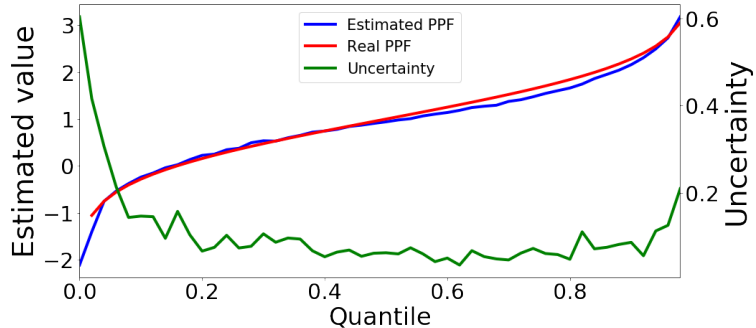


Figure 8: Reward distribution (red) predicted by a partially trained agent for an edible mushroom, compared to the actual distribution (blue). We see the agent has correctly learned the distribution. The per-quantile epistemic uncertainty on the predicted distribution is shown in green. We see the uncertainty concentrates on the lower quantiles, which are most affected when an agent makes a mistake.

We also examine the reward distributions learned by our agents, and use multiple samples of θ drawn using randomized MAP sampling to also study the per-quantile uncertainty. Specifically, in figure 8 we plot the reward distribution predicted by our agent for an edible mushroom. We see that the agent has correctly

learned the distribution. We also plot the per-quantile uncertainty on this distribution, $\mathbb{E}_{\theta}[y_i|\theta]$, estimated from 20 samples of θ . We observe that the per-quantile uncertainty provides important information: the agent is a lot less certain about the lower quantiles than the rest of the distribution. This is because the possibility of receiving a very negative reward if the model is wrong affects the lower quantiles much more than the upper quantiles.

E Locating the epistemic uncertainty in the distribution

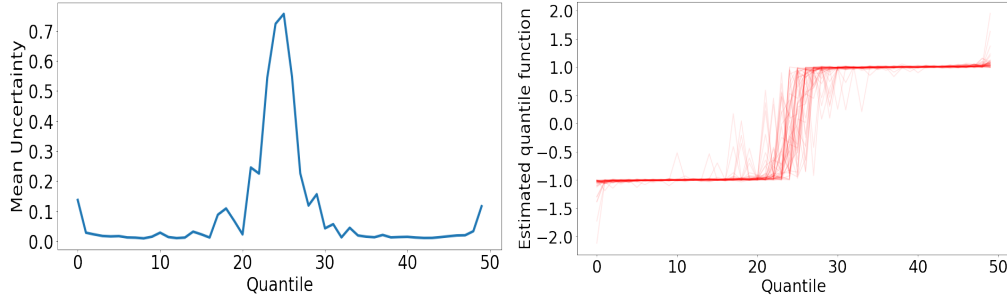


Figure 9: Locating the uncertainty on a probability distribution that produced ten 1 values and ten -1 values. Left: epistemic uncertainty on the values of the quantiles of this distribution. As expected, the uncertainty is larger on the middle quantiles. Right: probability point functions for these distributions, predicted by the 20 samples of the approximate posterior distribution over θ used to determine per-quantile uncertainties.

Here, we show that our Bayesian formulation of learning a distribution allows us to locate the uncertainty in the estimated distribution. We first produce 20 data points to be learned by our network, ten of which have a value of 1 and ten of which have a value of -1. With these samples, the epistemic uncertainty on the middle quantiles of the estimated distribution that produced these samples should be higher than that on the lower quantiles. For example, there are not enough data points to decide whether the median value should be 1 or -1. We obtain 20 samples of θ using the approximate MAP sampling procedure of [Pearce et al., 2018], and measure the per-quantile epistemic uncertainty using the observed standard deviation in the predictions.

Our experimental results are shown in figure 9. The epistemic uncertainty is indeed higher on the middle quantiles than on the other quantiles. This is reflected in the larger amount of noise in the predictions of the ensemble for those quantile values.

F Further results on Cartpole

We provide a visual representation of the predictions given by two networks with θ obtained by randomized MAP sampling in the Cartpole domain in figure 10. The different priors used in the approximate MAP scheme of [Pearce et al., 2018] forces diversity in the network predictions, which can be interpreted as an indication of the agent’s epistemic uncertainty. As we can expect, the epistemic uncertainty on the sub-optimal action is higher than for the better action (as witnessed by the larger difference between network predictions), since that action is selected less often in that state.

G Further results on the Atari suite

G.1 Tracking the epistemic uncertainty: experimental setup

Our experiment reproduces the training procedure of [Dabney et al., 2018b], except that we 1) use a network architecture allowing us to measure the epistemic uncertainty using randomized MAP sampling and 2) train our agent for 50 million steps instead of the usual 200 million due to computational limitations. Specifically, following [Osband et al., 2016], instead of having two separate networks, we have both networks

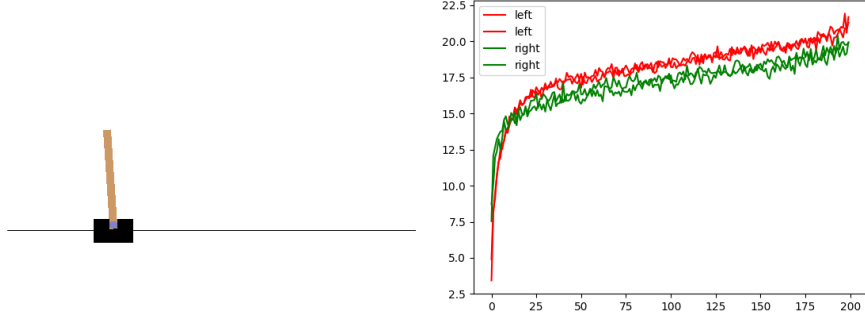


Figure 10: Left: state of the agent. Right: network predictions for the return distribution corresponding to the left action (red) and the right action (green), for two samples of θ drawn with randomized MAP sampling. Informally, $\tilde{\sigma}_{\text{epistemic}}$ stems from the difference in predictions between the two networks, and $\tilde{\sigma}_{\text{aleatoric}}$ correspond to the general trend in both predictions. In this case, the best action indeed corresponds to going left. The aleatoric uncertainty here comes from the fact that the agent does not know what the current time step is, so does not know precisely when the episode terminates.

share common parameters within a “body” consisting of convolutional layers, on top of which lie two “heads” with separate parameters, consisting of two linear layers, which each correspond to one of the networks. As in [Hafner et al., 2018] we only define a prior on the two heads, and we use the anchoring scheme of [Pearce et al., 2018] to enforce this prior. The outputs from both heads are averaged to produce the value estimates used by the policy. This different architecture did not lead to any noticeable difference in training compared to a baseline QR-DQN agent, except that training time increased by about 10% using a GPU.

G.2 Information Directed Sampling: experimental setup

Algorithm 2 Action selection with Information Directed Sampling

Input: State s and a set of possible actions \mathcal{A} .
for a in \mathcal{A} **do**
 Compute regret $\Delta(s, a) = \max_{a' \in \mathcal{A}} [\mu(s, a') + \lambda \tilde{\sigma}_{\text{epistemic}}(s, a')] - [\mu(s, a) - \lambda \tilde{\sigma}_{\text{epistemic}}(s, a)]$
 Normalize aleatoric uncertainty $\rho^2(s, a) = \tilde{\sigma}_{\text{aleatoric}}^2(s, a) / (\epsilon + \frac{1}{|\mathcal{A}|} \sum_{a'} \tilde{\sigma}_{\text{aleatoric}}^2(s, a'))$
 Compute information $I(s, a) = \log(1 + \frac{\tilde{\sigma}_{\text{epistemic}}^2}{\tilde{\sigma}_{\text{aleatoric}}^2}) + \epsilon$
 Compute regret-information ratio $\Psi(s, a) = \frac{\Delta^2(s, a)}{I(s, a)}$
end for
Output: $\text{argmax}'_a [\Psi(s, a)]$

To implement information directed exploration as in [Nikolov et al., 2019], we use the same network architecture as described above. Using our uncertainty estimates $\tilde{\sigma}_{\text{epistemic}}$ and $\tilde{\sigma}_{\text{aleatoric}}$, the agent selects actions using algorithm 2. In algorithm 2, λ is a hyperparameter that we set to 0.1 as in [Nikolov et al., 2019], and ϵ is set to 10^{-5} to prevent division by zero.

To compare our implementation of information directed exploration to QR-DQN and to Bootstrapped DQN, we reimplemented these algorithms within our code base and used the same values for all common parameters. Evaluation scores during training are shown in the main text, and average scores for the final trained agents are shown in table 1.

G.3 Exploration via Thompson sampling

We also report preliminary results of an experiment in which we train agents that select actions using Thompson sampling (in the same way as in the Cartpole environment) on the following Atari games: Alien, Amidar, Assault, Asterix, and Breakout. We train all agents for 50 million frames. Every 1M frames, these

Game	Human	QR-DQN	IDS	Bootstrapped
Alien	7128	1490 \pm 159	1670\pm64	1255 \pm 98
Amidar	1719	665 \pm 100	706 \pm 32	532 \pm 13
Assault	742	8452 \pm 910	6838 \pm 1679	2090 \pm 189
Asterix	8503	32105\pm4090	26625 \pm 6749	7134 \pm 217

Table 1: Comparison of average scores on Atari for the final trained agents for the three algorithms we consider, with standard deviations reported over 3 training seeds.

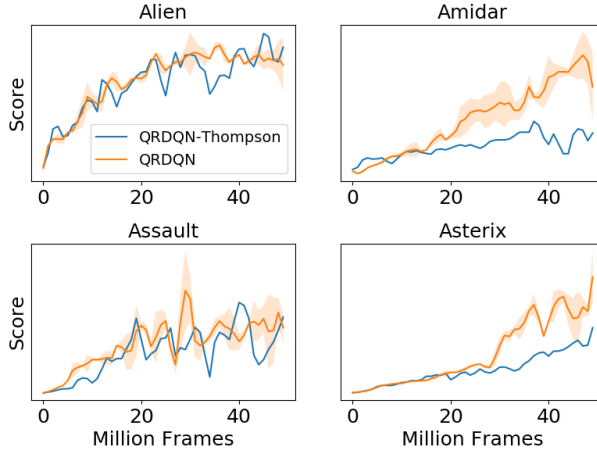


Figure 11: Evaluation results during training of QR-DQN agents with an ϵ -greedy policy and a QR-DQN agent that uses Thompson sampling with $\tilde{\sigma}_{\text{epistemic}}$.

agents are evaluated on 500k frames, as in [Mnih et al., 2015, Dabney et al., 2018b]. Table 1 shows the best evaluation results achieved during training for both our implementation of QR-DQN with an ϵ -greedy policy as in [Dabney et al., 2018b], and QR-DQN with a Thompson sampling policy using our uncertainty metric and our modified network architecture described above. Figure 11 shows evaluation scores during training, and table 2 shows the scores attained by final trained agents. Note that these figures correspond to three training seeds for QR-DQN with an ϵ -greedy policy, but only one seed for QR-DQN with Thompson sampling due to computational limitations.

Game	QR-DQN (ϵ -greedy)	QR-DQN (Thompson sampling)
Alien	1490 \pm 159	1549
Amidar	665\pm100	302
Assault	8452 \pm 910	10427
Asterix	32105\pm4090	20100
Breakout	565	515

Table 2: Comparison of scores on 5 Atari games obtained by a QR-DQN agent as in [Dabney et al., 2018b] and an agent that explores using Thompson sampling and $\tilde{\sigma}_{\text{epistemic}}$. Results for QR-DQN with Thompson sampling correspond to a single training seed.

We observe that agents that use Thompson sampling with our uncertainty metric all learn successful policies on these games. However, on some games agents that use Thompson sampling to select actions learn more slowly than the ϵ -greedy agent. This result is in line with our Cartpole results: the agents that use Thompson sampling spend more time exploring less rewarding parts of the MDP, and at the end of training lag behind the ϵ -greedy agents that have spent more time exploiting simple but successful policies (such as moving the paddle towards the ball in Breakout). We hypothesize that reducing the weight of the prior during learning may lead to more exploitative and thus more successful policies; we leave this to future work.